DRAFT VERSION FEBRUARY 1, 2008
Preprint typeset using LATEX style emulateapj v. 10/09/06

arXiv:0708.1215v1 [astro-ph] 9 Aug 2007

NEAR-FIELD MICROLENSING FROM WIDE-FIELD SURVEYS

CHEONGHO HAN
Program of Brain Korea 21, Institute for Basic Science Research, Department of Physics,
Chungbuk National University, Chongju 361-763, Korea; cheongho@astroph.chungbuk.ac.kr

Draft version February 1, 2008

ABSTRACT

We estimate the rate of near-field microlensing events expected from all-sky surveys and investigate the properties of these events. Under the assumption that all lenses are composed of stars, our estimation of the event rate ranges from $\Gamma_{\rm tot} \sim 0.2\ {\rm yr}^{-1}$ for a survey with a magnitude limit of $V_{\rm lim} = 12$ to $\Gamma_{\rm tot} \sim 20\ {\rm yr}^{-1}$ for a survey with $V_{\rm lim} = 18$. We find that the average distances to source stars and lenses vary considerably depending on the magnitude limit, while the dependencies of the average event time scale and lens-source transverse speed are weak and nearly negligible, respectively. We also find that the the average lens-source proper motion of events expected even from a survey with $V_{\rm lim} = 18$ would be $\langle\mu\rangle \gtrsim 40\ {\rm mas\ yr}^{-1}$, implying that the source and lens of a significant fraction of near-field events could be resolved from high-resolution follow-up observations. From the investigation of the variation of the event characteristics depending on the position of the sky, we find that the average distances to source stars and lenses become shorter, the lens-source transverse speed increases, and the time scale becomes shorter as the the galactic latitude of the field increases. Due to the concentration of events near the galactic plane, we find that $\gtrsim 50\%$ of events would be detected in the field with $b \leq 20^\circ$.

Subject headings: gravitational lensing

1. INTRODUCTION

The concept of one star gravitationally amplifying the light from another background star was first considered by Einstein (1936), although he concluded that the chance to observe this phenomenon (gravitational microlensing) would be very low. With the advance in technology, however, detections of microlensing events became feasible from systematic searches. The first detections were reported in the early 1990s (Alcock et al. 1993; Aubourg et al. 1993; Udalski et al. 1993). To date, lensing events are routinely detected with a rate of $\gtrsim 500$ events per season and the total number of detections now exceeds 3000. To maximize the number of detections, these searches have been and are being conducted toward very dense star fields of nearby galaxies such as the Magellanic Clouds (Alcock et al. 2000; Afonso et al. 2003) and M31 (Ansari et al. 1999; Calchi Novati et al. 2005; Uglesich et al. 2004; de Jong et al. 2004; Riffeser et al. 2003), and galactic center (Alcock et al. 2001; Hamadache et al. 2006; Sumi et al. 2006; Bond et al. 2001).

Recently, a detection of a lensing event occurred on a nearby star was reported by Gaudi et al. (2007) and Fukui et al. (2007). The star (GSC 3656-1328) is located about 1 kpc from the sun in the disk of the Milky Way. This detection along with the advent of transient surveys capable of covering a very wide field with high cadence such as ASAS (Szczygieł& Fabrycky 2007), ROTSE (Akerlof et al. 2003), TAROT and ARAGO (Boër 2001), and Pan-Starrs (Hodapp et al. 2004) have drawn attention of many researchers in microlensing community on the feasibility of near-field microlensing surveys. If near-field events could be detected from such surveys, they would be able to provide precious information about the matter distribution around the sun including dark objects. In addition, these surveys might enable detections of close planets with the microlensing technique that has demonstrated its capability in detecting distant planets (Bond et al. 2004; Udalski et al. 2005; Beaulieu et al. 2006; Gould et al. 2006).

The probability of lensing occurring on nearby stars has been estimated by Colley & Gott (1995) and Nemiroff (1998). The estimation of Colley & Gott (1995) focused on only events that could be observable with naked eyes, i.e. with a magnitude limit $V_{\rm lim} \sim 6$. Nemiroff (1998) estimated the lensing probability expected from surveys with various magnitude limits. However, he estimated the probability in terms of the average number of stars undergoing lensing magnification at a moment, not in terms of events per year, by using the combination of the star-count information and optical depth to lensing. The optical depth to lensing represents the probability that any given star is microlensed with a magnification $A \geq 1.34$ at any given time. This optical depth is dependent on the mass distribution but it is independent of the mass of the individual lensing objects. Therefore, the probability based on the optical depth does not provide detailed information about the physical parameters of lens systems such as the lens mass, locations of the lens and source, and their relative transverse speed, and the observables of events such as the event time scale and source brightness. For this information, additional modelling of the mass function and velocity distribution of galactic matter is required.

In this paper, we extend the works of Colley & Gott (1995) and Nemiroff (1998) to estimate the rate of lensing events in terms of event per year and to obtain the distributions of the physical parameters and observables of events expected from all-sky lensing surveys with various magnitude limits. For this, we conduct Bayesian simulation of near-field lensing events.

The paper is organized as follows. In § 2, describe the details of the simulation. In § 3, we present the resulting event rate and distributions of the physical parameters of lens systems and observables of lensing events. We also investigate the variation of the event characteristics and lensing probability depending on the position of the sky. We analyze the tendencies found in the distribution and explain the reasons for these tendencies. We summarize the result and conclude in § 4.

2. LENSING SIMULATION

To investigate the rate and properties of near-field lensing events expected to be detected from wide-field surveys, we conduct Bayesian simulation of these events. The basic scheme of the simulation is as follows.

1. We first produce source stars on the sky that can be seen from a survey with a given magnitude limit. We assign the locations on the sky and distances to stars based on a mass distribution model of the Galaxy. The stellar brightness is assigned based on a model luminosity function of stars considering distances to stars and extinction.

2. Once source stars are produced, we then produce lenses whose locations and masses are assigned based on models of the mass distribution and mass function, respectively.

3. To estimate the event rate in terms of events per year, it is required to model velocity distributions of source stars and lenses. The velocity distribution is also required to estimate the distributions of the physical parameters of lens systems and the observables of lensing events.

The details of the simulation are described in the following subsections.

2.1. *Stellar Distribution*

We model the mass distribution in the solar neighborhood as a double-exponential disk of the form

$$\rho(R,z) \propto \exp\left[-\left(\frac{R-R_0}{h_R}+\frac{|z|}{h_z}\right)\right], \qquad (1)$$

where R_0 is the galactocentric distance of the sun and h_R and h_z are the radial and vertical scale heights, respectively. We adopt $R_0 = 8$ kpc. For the radial scale height, we adopt a fixed value of $h_R = 4.0$ kpc. For the vertical scale heights, on the other hand, we adopt varying values depending on the stellar brightness such that $h_z = 117$ pc for $M_V \leq 2.0$, 195 pc for $M_V \leq 3.0$, 260 pc for $M_V \leq 4.0$, 325 pc for $M_V \leq 5.0$, 390 pc for $M_V \leq 6.0$, 455 pc for $M_V \leq 7.0$, and 520 pc for $M_V > 7.0$.

We model the luminosity function of stars by adopting that of stars in the solar neighborhood presented in Binney & Merrifield (1998). This luminosity function is constructed by combining the data published in Allen (1973) for $M_V \leq 0$, in Jahreiss & Wielen (1983) and Kroupa, Tout & Gilmore (1990) for $M_V > 0$.

Extinction is modeled such that the stellar flux decreases exponentially with the increase of the dust column density, i.e.

$$A_V = -2.5\log[\exp(-k\Sigma_{\rm d})], \qquad (2)$$

where $\Sigma_{\rm d}$ is the dust column density and k is a proportional constant. The dust column density $\rho_{\rm d}$ is computed on the basis of an expontial dust distribution model, i.e.

$$\Sigma_{\rm d} = \int_0^{D_{\rm S}} \rho_{\rm d}(\ell)d\ell, \qquad \rho_{\rm d} \propto \exp\left(-\frac{|z|}{h_{{\rm d},z}}\right), \qquad (3)$$

where the integral is along the line of sight toward the source star and $h_{{\rm d},z}$ is the vertical scale height of the dust distribution. We adopt $h_{{\rm d},z} = 150$ pc.

With these models, we produce source stars with their distances from the sun and locations on the sky assigned based on the mass distribution model and their absolute magnitudes allocated based on the luminosity function. Then, the apparent magnitude is computed based on the distance to the star and the amount of extinction. We set the normalization of the stellar number density and extinction so that the star count result from our simulation matches the star count data as a function of galactic latitude presented in Allen (1998).

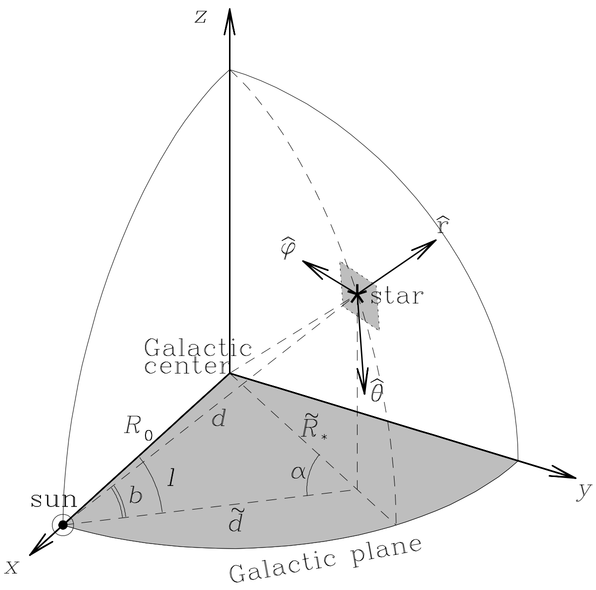

FIG. 1.— Position of a star as seen from the sun. (l,b) are the galactic longitude and latitude of the star, d is the distance to the star, and R_0 is the galactocentric distance of the sun. The vectors $\hat{\mathbf{r}}$, $\hat{\boldsymbol{\varphi}}$, and $\hat{\boldsymbol{\theta}}$ represent the unit vectors in the spherical coordinates centered at the position of the sun. The projected velocity of the star corresponds to $\mathbf{v}_{\perp} = v_{\varphi}\hat{\boldsymbol{\varphi}} + v_{\theta}\hat{\boldsymbol{\theta}}$.

2.2. *Lens Distribution and Mass Function*

In our simulation, we assume that only stars are responsible for lensing events and no MACHOs or stellar remnants are taken into consideration. For the mass function of lens matter, we adopt the model of Gould (2000) that is constructed based on the observations of Zoccali et al. (2000). The model has a double power-law distribution of the form

$$\frac{dN}{dm} = k\left(\frac{m}{m_c}\right)^{\gamma}; \qquad \gamma = \begin{cases} -2.0 & \text{for } m > m_{\rm c}, \\ -1.3 & \text{for } m < m_{\rm c}, \end{cases} \qquad (4)$$

where the turning-point mass is $m_{\rm c} = 0.7\ M_{\odot}$. The distance to the individual lenses are assigned from the same mass distribution model as that of source stars in equation (1). Since the lens is a star, its flux contributes to the observed flux. In this case, the flux from the lens works as blended flux to the observed flux. Then, the apparent magnification of an event appears to be lower than actual values (Nemiroff 1997). However, considering that source stars are bright enough to be monitored with small telescopes while most lenses are faint stars, the lens contribution to the observed flux is in most cases negligible (Han 1998).

2.3. *Velocity Distribution*

We model the velocity distribution as gaussian, i.e.

$$f(\mathbf{v}) \propto \exp\left[\frac{(\mathbf{v}-\bar{\mathbf{v}})^2}{2\sigma^2}\right]. \qquad (5)$$

The adopted means and standard deviations of the distributions of the individual velocity components in the galactocentric cylinderical coordinates are $(\bar{v}_R, \bar{v}_\phi, \bar{v}_z) = (0, 220, 0)$ km s^{-1}

and $(\sigma_R, \sigma_\phi, \sigma_z) = (38, 25, 20)$ km s^{-1}, respectively, i.e. a flat-rotating disk with gaussian velocity dispersion. For lensing, only the projected velocity, $\mathbf{v}_\perp$, as seen from the observer are related to lensing events. For lensing simulation, then, it is required to convert the velocity components into those in the spherical coordinates that are centered at the position of the sun. This conversion is done by the relation

$$\begin{pmatrix} v_r \\ v_\varphi \\ v_\theta \end{pmatrix} = \begin{pmatrix} \cos b & 0 & \sin b \\ 0 & 1 & 0 \\ -\sin b & 0 & \cos b \end{pmatrix} \begin{pmatrix} \cos\alpha & \sin\alpha & 0 \\ -\sin\alpha & \cos\alpha & 0 \\ 0 & 0 & 1 \end{pmatrix} \begin{pmatrix} v_R \\ v_\phi \\ v_z \end{pmatrix}, \qquad (6)$$

where b is the galactic latitude of the star and α is the angle between the two lines connecting the sun, the projected position of the star on the galactic plane, and the galactic center (see Figure 1). The angle α is related to the galactic longitude of the star (l), galactocentric distance of the sun, and the projected distance to the star on the galactic plane from the sun ($\tilde{d}$) by

$$\alpha = \sin^{-1}\left(\frac{R_0 \sin l}{\tilde{R}_\star}\right); \quad \tilde{R}_\star = (R_0^2 + \tilde{d}^2 - 2R_0\tilde{d}\cos l)^{1/2}, \qquad (7)$$

where $\tilde{R}_\star$ is the projected distance to the star from the galactic center (see Figure 1). Then, the projected velocity of a star depends not only on the galactic coordinates (l, b) but also on the distance to the star $d = \tilde{d}\sec b$, i.e. $\mathbf{v}_\perp = (v_\varphi, v_\theta) = \mathbf{v}_\perp(l, b, d)$. With the projected velocities of the lens, $\mathbf{v}_{\rm L} = \mathbf{v}_\perp(D_{\rm L})$, and source, $\mathbf{v}_{\rm L} = \mathbf{v}_\perp(D_{\rm S})$, the relative lens-source transverse velocity is computed by

$$\mathbf{v}_{\rm t} = \mathbf{v}_{\rm L} - \left[\mathbf{v}_{\rm S}\left(\frac{D_{\rm L}}{D_{\rm S}}\right) + \mathbf{v}_{\rm O}\left(\frac{D_{\rm S} - D_{\rm L}}{D_{\rm S}}\right)\right], \qquad (8)$$

where $\mathbf{v}_{\rm O}$ represents the projected velocity of the observer and $D_{\rm L}$ and $D_{\rm S}$ are the distances to the lens and source, respectively. We note that the observer, lens, and source are all in rotation with the same rotation speed, and thus the contribution of the rotation to the transverse speed is negligible. Then, the lens-source transverse motion is mostly caused by the dispersion of the rotation-subtracted residual velocity.

2.4. *Event Rate*

Once the source, lens, and their relative speed are chosen, its contribution to the event rate is computed by

$$\Gamma \propto n(l, b, D_{\rm S}) n(l, b, D_{\rm L}) D_{\rm S}^2 \sigma v_{\rm t}, \qquad (9)$$

where $n(l, b, d)$ represents the number density of stars at the position (l, b, d) and σ is the cross-section of the lens-source encounter. Here the factor $D_{\rm S}^2$ is included to account for the increase of the number of source stars with the increase of the distance. Under the definition of a lensing event as the approach of the source star within the Einstein ring of the lens (equivalently, source flux is magnified with a magnification $A \geq 1.34$), the lensing cross-section is set as $\sigma = 2r_{\rm E}$, where $r_{\rm E}$ is the physical Einstein ring radius. The Einstein radius is related to the physical parameters of the lens system by

$$r_{\rm E} = \left(\frac{4GM}{c^2}\right)^{1/2} \left[\frac{D_{\rm L}(D_{\rm S} - D_{\rm L})}{D_{\rm S}}\right]^{1/2}, \qquad (10)$$

where M is the mass of the lens. We assume that the survey is conducted all through the year[1] and events are detected with 100% efficiency.

TABLE 1
RATES OF MICROLENSING EVENTS

$V_{\rm lim}$	$N_{\star,\rm tot}$	$\langle\tau\rangle$	$\Gamma_{\rm tot}$ (yr^{-1})
12	0.14×10^7	0.16×10^{-8}	0.18
14	0.65×10^7	0.32×10^{-8}	0.61
16	2.4×10^7	0.60×10^{-8}	3.86
18	8.0×10^7	1.0×10^{-8}	21.20

NOTE. — Rates of near-field microlensing events, $\Gamma_{\rm tot}$, expected from all-sky surveys with various magnitude limits, $V_{\rm lim}$. Also listed are the total number of stars that can be monitored from the surveys, $N_{\star,\rm tot}$, and the average optical depth to lensing, $\langle\tau\rangle$.

3. RESULTS

In Table 1, we list the total event rate, $\Gamma_{\rm tot}$, expected from surveys with various magnitude limits. Also listed in the table are the total number of stars that can be monitored from the surveys, $N_{\star,\rm tot}$, and the average optical depth to lensing, $\langle\tau\rangle$. The optical depth is determined from the mass distribution model by

$$\tau(l, b) = \frac{\int_0^\infty dD_{\rm S} n(l, b, D_{\rm S}; V \leq V_{\rm lim}) D_{\rm S}^2 \int_0^{D_{\rm S}} dD_{\rm L} n(l, b, D_{\rm L}) r_{\rm E}^2}{\int_0^\infty dD_{\rm S} n(l, b, D_{\rm S}; V \leq V_{\rm lim}) D_{\rm S}^2}, \qquad (11)$$

where the factor $\int_0^\infty dD_{\rm S} n(l, b, D_{\rm S}; V \leq V_{\rm lim}) D_{\rm S}^2$ corresponds to the number of stars brighter than the magnitude limit toward the observational field, $N_\star$, and the other factor $\int_0^{D_{\rm S}} dD_{\rm L} n(l, b, D_{\rm L}) r_{\rm E}^2$ is the accumulation of the area occupied by the Einstein rings of the individual lenses along the line of sight toward the source star. We note that although there exists limitation in the brightness of source stars ($V < V_{\rm lim}$), there is no restriction in the lens brightness. The presented value in Table 1 are the mean optical depth averaged over the whole sky, i.e. $\langle\tau\rangle = (4\pi)^{-1} \int_{-180^\circ}^{180^\circ} dl \int_{-90^\circ}^{90^\circ} \tau(l, b) \sin b \; db$, and the total number of stars over the entire sky, i.e. $N_{\star,\rm tot} = \int_{-180^\circ}^{180^\circ} dl \int_{-90^\circ}^{90^\circ} N_\star(l, b) \sin b \; db$. We find that our estimation of the optical depth matches well with the estimation of Nemiroff (1998). The multiplication $N_{\star,\rm tot} \times \langle\tau\rangle$ represents the number of stars undergoing lensing magnification at a given moment, which was presented in Nemiroff (1998). We also find a good match between his and our estimations. The estimated event rate ranges from $\Gamma_{\rm tot} \sim 0.2$ per year for a survey with a magnitude limit of $V_{\rm lim} = 12$ to $\Gamma_{\rm tot} \sim 20$ per year for a survey with $V_{\rm lim} = 18$, confirming the result of Nemiroff (1998) that the lensing probability rapidly increases with the increase of the magnitude limits. Two factors contribute to the increase of the event rate with the increase of the magnitude limit. The first factor is the increase of the number of source stars and the other factor is the increase of the line of sight toward source stars and thus increase of the optical depth. We find that the former factor is more important.

In Figure 2, we present the distributions of lens parameters and the observables of events. From the top, the individual panels represent the distributions of the source star brightness, distances to source stars and lenses, lens-source transverse speed, event time scale, and lens-source relative proper motion, respectively. The event time scale is determined by the Einstein time scale, which is required for the source to transit the Einstein radius of the lens, i.e. $t_{\rm E} = r_{\rm E}/v$. The proper motion corresponds to $\mu = \theta_{\rm E}/t_{\rm E}$, where $\theta_{\rm E} = r_{\rm E}/D_{\rm L}$ is the angular Einstein radius. In Table 2, we also present the average

---

[1] This requires a network of wide-field telescopes distributed over the Earth.

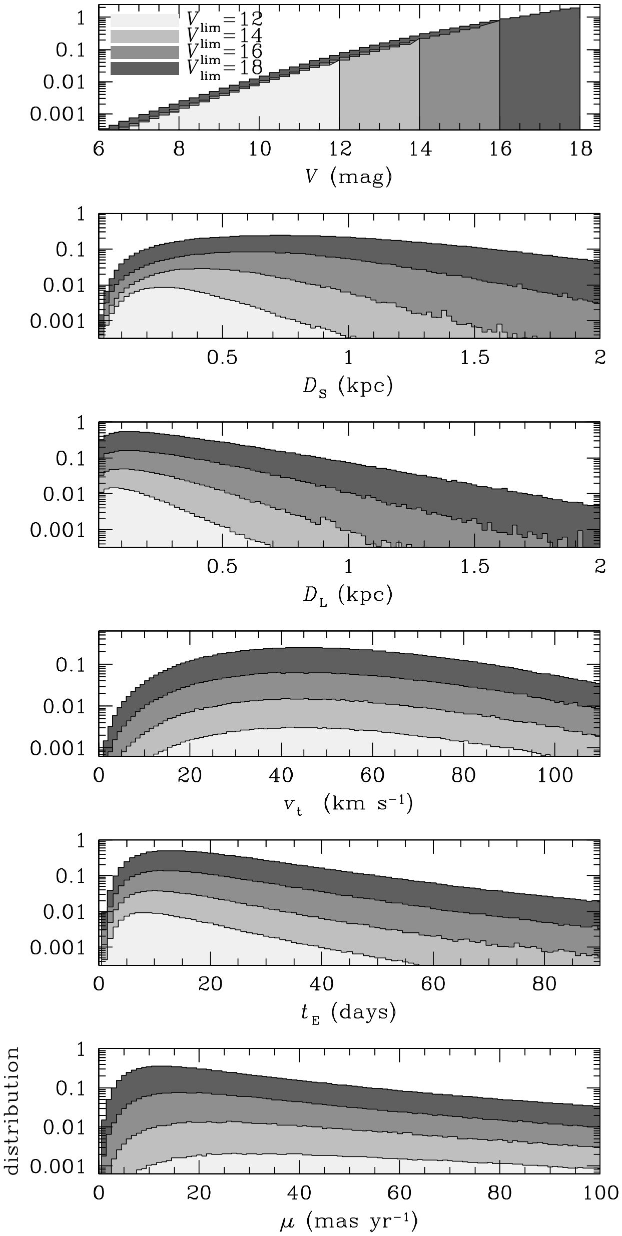

FIG. 2.— Distributions of lens parameters and observables of near-filed microlensing events expected from all-sky surveys with various magnitude limits, $V_{\rm lim}$. From the top, the individual panels represent the distributions of the source star brightness (V), distances to the source star ($D_{\rm S}$) and lens ($D_{\rm L}$), transverse speeds ($v_{\rm t}$), event time scale ($t_{\rm E}$), and lens-source relative proper motions (μ), respectively. The mean values of the parameters and observables are listed in Table 2.

values of the lens parameters. From Figure 2 and Table 1 and 2 we find the following tendencies.

1. The distributions of $D_{\rm S}$ and $D_{\rm L}$ vary considerably depending on the magnitude limit. The trend, as expected, is that the distances to the source and lens become larger as fainter stars are monitored.
2. On the other hand, the dependency of the distribution of $t_{\rm E}$ on the magnitude limit is not very strong and the dependency of the velocity distribution is nearly negligible.
3. With the increase of the magnitude limit, the distance to the lens increases while the transverse speed remains nearly the same. As a result, the average proper motion $\mu = \theta_{\rm E}/t_{\rm E} = v_{\rm t}/D_{\rm L}$ of events decreases as the magnitude limit increases. However, we note that even for surveys with $V_{\rm lim} \sim 18$, the mean proper motion of events is $\langle\mu\rangle \gtrsim 40$ mas yr^{-1}, which is much larger than the typical value of 5 mas yr^{-1} of galactic bulge events. Then, the lens and source of a significant fraction of near-field events can be resolved from follow-up observations by using high-resolution instrument such as the *Hubble Space Telescope* conducted several years after the peak of the magnification. This not only enables the measurement of the proper motion but also helps to identify the lens.

TABLE 2
AVERAGE VALUES OF LENS PARAMETERS

$V_{\rm lim}$ (mag)	$\langle D_{\rm S}\rangle$ (kpc)	$\langle D_{\rm L}\rangle$ (kpc)	$\langle v_{\rm t}\rangle$ (km s^{-1})	$\langle t_{\rm E}\rangle$ (days)	$\langle\mu\rangle$ (mas yr^{-1})
12	0.39	0.19	55.3	18.7	71.5
14	0.56	0.27	55.4	21.9	58.5
16	0.78	0.36	55.6	25.0	49.1
18	1.03	0.44	56.0	27.4	44.1

NOTE. — Average values of the lens parameters and observables of near-field microlensing events expected from wide-field surveys with various magnitude limits, $V_{\rm lim}$.

Figure 3 shows the variation of the event characteristics and probability of lensing depending on the position of the sky. From the top, the panels in each column represent the distributions of the average distances to source stars and lenses, lens-source transverse speed, event time scale, number density of stars in the field, optical depth, and the event rate per unit angular area of the sky. The panels in each row represent the distributions for different magnitude limits. The tendencies found from the maps are as follows.

1. For a survey with a given magnitude limit, the average distances to source stars and lenses become smaller as the latitude of the field increases. This is because the number density of stars along the line of sight decreases more rapidly as the field is located further away from the disk plane.
2. The transverse speed increases with the increase of the latitude. This tendency is due to the elongation of the velocity ellipsoid of the rotation-subtracted residual stellar motion. The major axes of the velocity ellipsoid are $(\sigma_R, \sigma_\phi, \sigma_z) = (38, 25, 20)$ km s^{-1} and thus the ellipsoid is elongated more along the galactic plane than along the pole direction. Then, the dispersion of the projected velocity distribution for stars located toward the direction of the galactic plane is $\sigma_\perp(b=0^\circ) = (\sigma_\phi^2+\sigma_z^2)^{1/2} \sim 32$ km s^{-1}, while the velocity dispersion for stars located toward the galactic pole direction is $\sigma_\perp(b=90^\circ) = (\sigma_R^2+\sigma_\phi^2)^{1/2} \sim 45$ km s^{-1}. This also explains the tendency of the longer time scales for events occurred on stars located at a lower latitude.
3. With the increase of the stellar number density combined with the increase of the optical depth, the event rate increases rapidly toward the galactic plane. We find that $\gtrsim 50\%$ of events are expected to be found in the fieled with $b \leq 20^\circ$.

FIG. 3.— Variation of the characteristics and probability of near-field microlensing events depending on the position of the sky. From the top, the panels in each column represent the distributions of the average distances to source star ($D_{\rm S}$) and lens ($D_{\rm L}$), lens-source transverse speed ($v_{\rm t}$), event time scale ($t_{\rm E}$), average number density of stars in the field ($N_\star$), optical depth (τ), and the event rate per unit angular area (Γ). The panels in each row represent the distributions for different magnitude limits. The map is centered centered at the galactic center, i.e. $(l,b) = (0^\circ, 0^\circ)$.

4. CONCLUSION

Instigated by the recent discovery of an event occurred on a nearby star, we estimated the rate of near-field lensing events expected from all-sky surveys with various magnitude limits. Under the assumption that all lenses are composed of stars, our estimation of the event rate ranges from $\Gamma_{\rm tot} \sim 0.2$ per year for a survey with a magnitude limit of $V_{\rm lim} = 12$ to $\Gamma_{\rm tot} \sim 20$ per year for a survey with $V_{\rm lim} = 18$, confirming the previous result that lensing probability rapidly increases with the increase of the magnitude limit. The increase of the rate is due to two factors which are the extension of the line of the sight toward source stars and the increase of the number of source stars. We found that the latter factor is more important. We also investigated the distributions of the physical parameters of lens systems and the observables of these events. From this, we found that although the average distances to source stars and lenses vary considerably depending on the magnitude limit, the dependencies of the average event time scale and lens-source transverse speed are weak and nearly negligible, respectively. We also found that the the average lens-source proper motion of events expected from a survey with $V_{\rm lim} = 18$ would be $\langle\mu\rangle \gtrsim 40$ mas yr^{-1} and the value further increases as the magnitude limit becomes lower. This implies that the source and lens of a typical near-field lensing event can be resolved from high-resolution follow-up observations conducted several years after the peak of the lensing magnification. From the investigation of the variation of the event characteristics depending on the position of the sky, we found that the average distances to source stars and lenses become shorter, the lens-source transverse speed increases, and the time scale becomes shorter as the the galactic latitude of the field increases. Due to the concentration of events near the galactic plane, we found that $\gtrsim 50\%$ of events would be detected in the field with $b \leq 20^\circ$.

This work was supported by the research grant of Chungbuk National University in 2007.

REFERENCES

Afonso, C., et al. 2003, A&A, 400, 951
Akerlof, C. W., et al. 2003, PASP, 115, 132
Alcock, C., et al. 1993, Nature, 365, 621
Alcock, C., et al. 2000, ApJ, 542, 281
Alcock, C., et al. 2001, ApJ, 557, 1035
Allen, C. W. 1973, Astrophysical Quantities, third edition (London: Athlone Press)
Allen, C. W. 1998, Astrophysical Quantities, fourth edition (London: Athlone Press), 482
Ansari, R., et al. 1999, A&A, 344, L49
Aubourg, E., et al. 1993, Nature, 365, 623
Beaulieu, J. P., et al. 2006, Nature, 439, 437
Binney, J., & Merrifield, M. 1998, Galactic Astronomy (Princeton: Princeton University Press), 124
Boër, M. 2001, Astronomische Nachrichten, 322, 343
Bond, I. A., et al. 2001, MNRAS, 327, 868
Bond, I.A., et al. 2004, ApJ, 606, L155
Calchi Novati, S., et al. 2005, A&A, 443, 911
Colley, W. N., & Gott, J. R. 1995, ApJ, 452, 82
de Jong, J. T. A., et al. 2004, A&A, 417, 461
Einstein, A. 1936, Science, 84, 506
Fukui, A., et al. 2007, preprint (arXiv:0708.1066v1)
Gaudi, B. S., et al. 2007, ApJ, submitted
Gould, A. 2000, ApJ, 535, 928
Gould, A., et al. 2006, ApJ, 644, L37
Han, C. 1998, ApJ, 500, 569
Hamadache, C., et al. 2006, A&A, 454, 185
Hodapp, K. W., et al. 2004, Astronomische Nachrichten, 325, 636
Jahreiss, H., & Wielen, R. 1983, The Nearby Stars and Stellar Luminosity Function, IAU Colloquium 76, eds. A. G. D. Philip & A.R. Upgren (Schenectady: L. Davis Press), 227
Kroupa, P., Tout, C. A., & Gilmore, G. 1990, MNRAS, 244, 76
Nemiroff, R. J. 1997, ApJ, 486, 693
Nemiroff, R. J, 1998, ApJ, 509, 39
Riffeser, A., Fliri, J., Bender, R., Seitz, S., & Gössl, C. A. 2003, ApJ, 599, L1
Sumi, T., et al. 2006, ApJ, 636, 240
Szczygieł, D. M., & Fabrycky, D. C. 2007, MNRAS, 377, 1263
Udalski, A., Szymański, M., Kałużny, J., Kubiak, M., Krzemiński, W., Mateo, M., Preston, G. W., & Paczyński, B. 1993, Acta Astronomica, 43, 289
Udalski, A., et al. 2005, ApJ, 628, L109
Uglesich, R. R., Crotts, A. P. S., Baltz, E. A., de Jong J., Boyle, R. P., & Corbally, G. J. 2004, ApJ, 612, 877
Zoccali, M., Cassisi, S., Frogel, J. A., Gould, A., Ortolani, S., Renzini, A., Rich, R. M., & Stephens, A. W. 2000, ApJ, 530, 418

This figure "fig3.jpg" is available in "jpg" format from:

http://arXiv.org/ps/0708.1215v1